Pion production, pion absorption, and nucleon properties in dense nuclear matter: Relativistic Dirac-Brueckner approach at intermediate and high energies

Bernard ter Haar and Rudi Malfliet
Kernfysisch Versneller Instituut, University of Groningen, 9747 AA Groningen, The Netherlands
(Received 7 May 1987)

Within the relativistic Dirac-Brueckner approach we discuss the properties of highly-energetic nucleons and deltas in dense nuclear matter. The effective NN and NΔ interactions are constructed in a fully self-consistent way and reproduce all known properties of nuclear matter. We calculate the nucleon self-energy and the density-dependent effective NN and NΔ cross sections in a nuclear medium. Results show a sizable reduction of the Δ (pion) production cross section and important changes in the Δ absorption cross sections.

I. INTRODUCTION

Whether the pion can be taken as a useful tool for the study of relativistic heavy-ion collision processes has been the subject of extensive investigation over the last years.[1] The idea has been raised that the measured pion yield is strongly related to the equation of state of nuclear matter at the highest densities reached in this type of collision.[2] First calculations showed that the pion data could be explained by assuming a stiff equation of state of nuclear matter.[3] More recently, it has been realized, however, that these calculations lack several important microscopic ingredients. First, the equation of state was expressed in terms of a momentum-independent mean field. However, it is well known from the optical model and several microscopic calculations[4,5] that the single-particle "potential" or mean field exhibits a strong momentum dependence. As a result of this dependence, already at much lower densities than was thought, the nuclear medium behaves in a "stiff" fashion. Very recently, calculations with the Vlasov-Uhlenbeck-Uehling (VUU) approach indeed show a crucial influence of the momentum dependence of the mean field on the resulting equation of state.[6] Secondly, in all calculations performed so far the intrinsic medium (and density) dependence of the pion production and absorption mechanism has been ignored, for the simple reason that very little is known about this dependence. There are clear indications that the nucleon mean free path, or related to this, the elastic nucleon cross section in a nuclear medium, is density dependent.[7] It is therefore very plausible that also in the inelastic nucleon cross section, and thus in the pion production cross section, a similar medium dependence should be accounted for. It is our aim here to calculate the microscopic properties of highly energetic nucleons and pions in a dense nuclear medium. Incorporation of these results, for the mean field on one hand and for the density dependent "cross sections" on the other, calls into question the basic concepts of the kinetic equations that have been applied so far in the description of nucleus-nucleus collisions. This problem has been studied elsewhere,[8] resulting in the so-called Brueckner-Boltzmann equation, which consistently incorporates all the medium effects that a microscopic theory like the Brueckner one yields.

Knowledge of the properties of energetic nucleons and pions in the nuclear medium has a wider range of applicability than only in the calculation of relativistic nucleus-nucleus reactions. Within the framework of a local-density approximation, they apply as well to the field of proton-nucleus and pion-nucleus reactions. It is generally assumed that the $\Delta(\frac{3}{2},\frac{3}{2})$ resonance plays a major role in the description of the interaction of a pion with a nuclear medium. We shall use this knowledge and shall focus on the behavior of the Δ inside nuclear matter more than on the pion itself. With respect to elastic proton-nucleus scattering, it has been demonstrated recently that all observables are nicely reproduced within a relativistic Dirac approach,[9] yielding a single-particle interaction which consists of large Lorentz scalar and vector fields. These foregoing arguments support the approach that we present here, the relativistic Dirac-Brueckner (DB) approach for nucleons and deltas.

The starting point of our DB approach is given by a coupled set of t-matrix equations, by which the vacuum nucleon-nucleon (NN) and nucleon-delta (NΔ) interactions are calculated on the basis of relativistic one-boson-exchange (OBE) potentials. In this coupled-channel approach all elastic and inelastic NN observables can be reproduced reasonably well up to a (laboratory) energy of about 800 MeV. The next step in the approach is the transformation of the t-matrix equations, in accordance with Brueckner nuclear matter theory, to incorporate many-body effects on the effective NN and NΔ interactions. In a fully-self-consistent approach, both for the nucleon and the delta, we have been able to reproduce rather accurately the empirically known saturation properties of nuclear matter. In fact, the model predicts nucleon (and delta) properties for momenta below as well as above the nuclear Fermi level. The properties above the Fermi sea can be expressed in terms of an optical potential, and it turns out that agreement can be obtained with empirical values for nucleon energies below 300 MeV. All these results have been presented elsewhere.[10]

Here we shall focus on the properties of highly-

energetic nucleons and deltas in dense nuclear matter. We calculate the density-dependent effective NN and NΔ interactions in the same energy region as we did for free spacing scattering, i.e., nucleon energies below 1 GeV. For the nucleonic single-particle interaction we observe strong Lorentz scalar and vector components, in agreement with recent calculations for proton-nucleus scattering below a laboratory energy of 1 GeV. The two-body properties will be expressed by means of effective cross sections. While the vacuum cross sections are determined by the absolute square of t-matrix elements, their counterparts, the effective cross sections, are determined by the Dirac-Brueckner "G-matrix" elements. The legitimacy of this concept has been proven in the derivation of the above mentioned Brueckner-Boltzmann kinetic equation,[8] where the Boltzmann collision terms indeed depend on the G matrix. By this concept of effective cross sections we can demonstrate rather easily the density dependence of the different interactions. It will turn out, for example, that the NN→NΔ interaction is very seriously quenched at high densities. Since pion production is assumed to occur by means of this interaction, followed by the decay of the delta, this indicates a strong density dependence of pion production. Similar observations are made for the NΔ→NN and NΔ→NΔ reactions, which may give new insight into pion absorption (for which the theoretical situation is still very unclear[11]), and elastic pion scattering reactions.

In Sec. II we shall briefly explain our Dirac-Brueckner model. For a more extensive description, we refer to Ref. 10. In Sec. III, results on highly-energetic nucleons will be presented, while Sec. IV does the same for the nucleon-delta interactions. Conclusions are drawn in Sec. V.

II. THE RELATIVISTIC DIRAC-BRUECKNER APPROACH FOR NUCLEONS AND DELTAS

The DB approach is the outcome of work that was started by Walecka and co-workers[12] for schematic NN interactions. It has been extended to the case of realistic interactions by Shakin *et al.*[13] and Machleidt and Brockmann.[14] In Ref. 10 we incorporated delta degrees of freedom in the model. There are a couple of reasons for doing so. In the first place it was well known that the Δ-intermediate states are responsible for part of the attraction in the NN force (represented by exchange of an effective scalar meson) and, furthermore, for pseudoresonance structure in several phase shifts above 300 MeV.[15] Thus, for correctly describing the NN interaction, Δ degrees of freedom are necessary. This is particularly the case for nuclear matter calculations, since intermediate Δ states will behave differently from intermediate nucleon states inside nuclear matter. This might cause serious differences in the effective NN interaction. Besides, the behavior of a Δ inside nuclear matter is an interesting subject on its own.

At the heart of our calculation of the effective interactions in the (N,Δ) system lies a set of four coupled "G-matrix" equations:

$$\Gamma_{11}=V_{11}+\int\Gamma_{11}g_1^*V_{11}+\int\Gamma_{12}g_2^*V_{21}\ , \tag{2.1}$$

$$\Gamma_{12}=V_{12}+\int\Gamma_{11}g_1^*V_{12}+\int\Gamma_{12}g_2^*V_{22}\ , \tag{2.2}$$

$$\Gamma_{21}=V_{21}+\int\Gamma_{21}g_1^*V_{11}+\int\Gamma_{22}g_2^*V_{21}\ , \tag{2.3}$$

$$\Gamma_{22}=V_{22}+\int\Gamma_{21}g_1^*V_{12}+\int\Gamma_{22}g_2^*V_{22}\ , \tag{2.4}$$

where 1 (2) stands for the NN (NΔ) channel. The effective interactions (or relativistic G matrices) are represented by Γ_{ij}. We choose V_{ij} to be of a one-boson-exchange form, including vertex form factors. The "dressed" two-particle propagators are represented by g_i^*. Equations (2.1)–(2.4) are solved in a three-dimensional reduced form of the fully covariant ladder Bethe-Salpeter equation, including only positive-energy particles. One notices that in this set of equations the intermediate ΔΔ channel is ignored. The main reason for this is simplicity. Furthermore, because of the existing uncertainty in the meson coupling to the ΔΔ vertex, already reflected in V_{22},[10] we do not expect that an *ad hoc* inclusion of the intermediate ΔΔ channel would significantly improve the accuracy of our results. All the OBE parameters are fitted to elastic and inelastic NN observables for energies below 1 GeV, and are given in Ref. 10. For the NΔ→NΔ interaction, V_{22}, we included here only the "exchange" contribution, for which only the meson couplings to the NΔ vertex are important. The "dressed" two-particle propagators, g_i^*, are related to the single-particle propagators G_N^* and G_Δ^*. Most characteristic of the DB approach is the treatment of the dressed nucleon propagator, G_N^*. This propagator is determined by solving the Dyson equation:

$$G_N^*(k)=G_N^0(k)+G_N^0(k)\Sigma_N(k)G_N^*(k)\ , \tag{2.5}$$

where $G_N^0(k)$ can be written as $(\not k-m_N)^{-1}$. The formal solution of Eq. (2.5) is

$$G_N^*=[\not k-m_N-\Sigma_N(k)]^{-1}\equiv(\not k^*-m^*)^{-1}\ , \tag{2.6}$$

where we used a Lorentz expansion of the nucleon self-energy $\Sigma_N(k)$:

$$\Sigma_N(k)=\Sigma_s(k)-\gamma^0\Sigma_0(k)+\boldsymbol{\gamma}\cdot\mathbf{k}\Sigma_v(k)\ , \tag{2.7}$$

from which the definitions of m^* and k_μ^* trivially follow:

$$\begin{aligned} m^*&=m_N+\Sigma_s(k)\ ,\\ k_0^*&=k_0+\Sigma_0(k)\ ,\\ \mathbf{k}^*&=\mathbf{k}[1+\Sigma_v(k)]\ . \end{aligned} \tag{2.8}$$

This nucleon self-energy in the Brueckner model is determined by the effective interaction Γ_{11} [Eq. (2.1)], according to

$$\Sigma_N(k)=-i\int[\mathrm{tr}(G_N^*\Gamma_{11})-G_N^*\Gamma_{11}]\ . \tag{2.9}$$

The inclusion of Δ degrees of freedom does not change the essential features of the DB model, and full details can be found in Ref. 10. For reasons of completeness we sketch some of the ingredients involved.

For unstable particles like the Δ, the propagator becomes a complex quantity, on account of the virtual cou-

pling of the Δ to its decay channel(s). This "dressed" propagator is found by solving a Dyson equation, which for the Δ case is (see Fig. 1)

$$G_{\Delta}^{\mu\nu}=(G_{\Delta}^{0})^{\mu\nu}+(G_{\Delta}^{0})^{\mu\rho}\Sigma_{\rho\tau}^{\Delta}G_{\Delta}^{\tau\nu} , \tag{2.10}$$

where G_{Δ} and G_{Δ}^{0} denote the dressed and bare Δ propagator and Σ^{Δ} gives the irreducible Δ self-energy contribution. As indicated in Fig. 1, we have restricted the self-energy term, Σ^{Δ}, to the Nπ "bubble" and the Nρ "bubble." The formal solution of Eq. (2.10) is

$$\{G_{\Delta}\}^{-1}=\{G_{\Delta}^{0}-\Sigma^{\Delta}\}^{-1} , \tag{2.11}$$

where we have omitted all the indices.

The self-energy has usually negative real and imaginary components. The negative real part leads to a "physical" mass of the particle that is lower than the "bare" mass, which would be the mass of the particle in the absence of any decay channel. The imaginary part is directly connected to the physical decay width. Commonly, the unstable nature of a particle is treated in the quasiparticle formalism, in which the physical mass of the particle is taken as the relevant mass parameter, except in the particle propagator, where the full complex energy expression is used, either by including the self-energy as specified above, or in an approximate form, by the use of a complex mass: $\mu_{\Delta}=m_{\Delta}-i\Gamma/2$, where both m_{Δ} and Γ are the physical quantities.

The bare Δ mass m_0 is unknown and enters the self-energy calculations as a parameter that is adjusted in a comparison of the full dressed propagator with experimental data, specifically with the P_{33} πN scattering amplitudes. We fitted the P_{33} phase shift in combination with all the NN-scattering data. m_0 is not used as an input parameter, but is fixed such that the P_{33} phase shift has the correct resonance position: $m_{\Delta}=1.23$ GeV/c^2.

The self-energy of the Δ in nuclear matter consists now of two parts: Σ^{d}, the decay Δ self-energy which arises from virtual coupling of the bare Δ state with its decay channel, and Σ^{m}, the proper medium Δ self-energy that is the consequence of the coupling of the Δ to the nucleonic Fermi sea. These contributions are diagrammatically displayed in Fig. 2. The dressed Δ propagator G_{Δ}^{*} is given by Eq. (2.10), with the definition

$$\Sigma^{\Delta}=\Sigma^{m}+\Sigma^{d} . \tag{2.12}$$

The magnitude of the decay self-energy, Σ^{d}, in nuclear matter differs significantly from its vacuum value for two reasons: the fact that in the medium the Δ couples to a virtual dressed nucleon (instead of a "bare" nucleon), and, furthermore, the explicit effect of Pauli blocking.

The decay self-energy, Σ^{d}, contains a strong off-shell dependence; however, in the Brueckner scheme that we apply here, the medium self-energies are calculated for

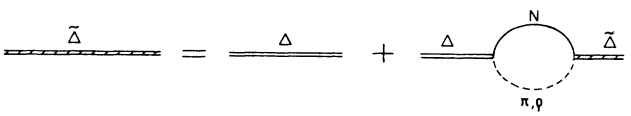

FIG. 1. Diagrammatic representation of the Dyson equation for the "dressed" Δ propagator.

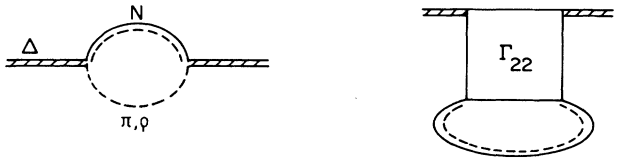

FIG. 2. Diagrammatic representation of the Δ self-energy contributions. The first diagram shows the coupling of the Δ to the ρN and πN "bubble," the second shows the Brueckner self-energy contribution.

on-shell dressed particles. Therefore we calculate Σ^{m} in a similar way as the nucleon self-energy [Eq. (2.9)],

$$\Sigma^{m}(E_k,k)=\sum_{k\le k_F}\langle \mathbf{k}\mathbf{k}' \mid \Gamma_{22} \mid \mathbf{k}\mathbf{k}'\rangle . \tag{2.13}$$

The solution for G_{Δ}^{*} is complicated by the fact that the Lorentz structure of G_{Δ}^{0} is more complex than its nucleon counterpart. Therefore, we cannot write equivalent expressions, as in Eqs. (2.6)–(2.8). So far, we have left the full solution for $G_{\Delta}^{*}(k)$ for the future, and opted for a more conventional approach, in which $\Sigma_{\Delta}=\Sigma^{d}+\Sigma^{m}$ is approximated by a purely scalar quantity.

In an iterative procedure, where Γ_{ij} depends on Σ_{N} and Σ_{Δ}, and vice versa, the model is made fully self-consistent, both with respect to nucleon and delta degrees of freedom. One should notice that, within the DB approach, the dependence of Γ_{ij} on Σ_{N}, in particular, goes further than in conventional Brueckner calculations. The reason for this is the following. The dressed on-shell nucleons can be represented by Dirac plane waves:

$$u^{*}(p,s)=\left[\frac{E^{*}+m^{*}}{2m^{*}}\right]^{1/2}\begin{bmatrix}1\\ \dfrac{\sigma\cdot\mathbf{k}^{*}}{E^{*}+m^{*}}\end{bmatrix}\chi_s , \tag{2.14}$$

where E^{*} has been defined by, $E^{*}=(\mathbf{k}^{*2}+m^{*2})^{1/2}$. Since m^{*} attains much lower values than the vacuum value, m_{N}, and (approximately) $\mathbf{k}^{*}$ equals $\mathbf{k}$, one sees that the lower components of this Dirac spinor are enhanced compared to the vacuum spinor. This has immediate consequences for the OBE interactions, V_{ij}, and thus also for Γ_{ij}. The fact that the DB approach yields better saturation properties than conventional Brueckner calculations is a result of this phenomenon. In particular, in V_{11} the scalar meson exchange is reduced by the enhanced lower Dirac components, which results in a lower attraction, while the vector meson exchange is enlarged, resulting in greater repulsion. Similar observations can be made for the other interactions V_{ij}. For example, the πNΔ vertex is also reduced by enhanced lower Dirac components of the nucleon.

As a result a self-consistent model is presented here based on a coupled set of equations of all effective t matrices (Γ_{11}, Γ_{12}, Γ_{21}, and Γ_{22}) supplemented by equations defining the self-energy of the nucleon and of the Δ. The OBE interactions between nucleons and deltas are determined from vacuum calculations and their parameters

are given in Ref. 10. Hence this approach to nuclear matter does not contain any additional free parameters.

III. NUCLEON-NUCLEON INTERACTIONS ABOVE THE FERMI SURFACE

A. Medium properties of highly-energetic nucleons and deltas

The full DB model, including Δ degrees of freedom, presented in Sec. II, enables us to perform calculations for high nucleon momenta. As a first result, the scalar and vector parts of the nucleon self-energy, Σ_s and Σ_0, are shown at normal density, for a broad momentum range, in Fig. 3. The values obtained are comparable to those obtained theoretically or empirically from high-energy proton-nucleus collisions.[16,17] In this figure, our DB results (solid lines) are compared to sophisticated field-theoretic calculations in the relativistic impulse approximation by Tjon and Wallace.[17] The equivalence is very remarkable. Both calculations are based on a one-boson-exchange interaction that has been fitted to free NN observables for energies below 1 GeV. Our calculation incorporates, self-consistently, medium effects in the t matrix for dressed positive-energy nucleons only. The calculation of Tjon and Wallace is not self-consistent but incorporates "bare" negative-energy states of the nucleon. Although these physical concepts are very different, the calculations are somehow related in the sense that "dressed" positive-energy states can be expanded in "bare" positive-energy and negative-energy states. It might be clear from the magnitude of the self-energy components that self-consistency is an important requirement and we calculated that it may change the values of Σ_s and Σ_0 by about 70–100 MeV. This may indicate that the intriguing question about the influence of negative-energy nucleon states has not been settled as yet and needs more investigation.

A rather complete survey of our results on the nucleon self-energy is given in Table I. Here, for several densities, all complex self-energy components are presented, together with values for the "mean-field" U, and the resulting single-particle energy. In nuclear matter the single-particle energy is given by

$$E_{\text{s.p.}}=[k^2(1+\Sigma_v)^2+(m_N+\Sigma_s)^2]^{1/2}-\Sigma_0-m_N\ , \tag{3.1}$$

where only the real part of $\Sigma(k)$ is included.

The difference between $E_{\text{s.p.}}$ and E_{free}, the latter defined by

$$E_{\text{free}}=(k^2+m_N{}^2)^{1/2}-m_N\ , \tag{3.2}$$

gives the real part of the "mean-field" $U(k)$. One clearly sees that U has a strong dependence on both the nuclear matter density, as well as on the nucleon momentum. These properties of U have been described more extensively elsewhere.[8]

Also, the Δ is dressed dynamically, i.e., it has a vacuum self-energy, which is such that the vacuum-dressed Δ corresponds to the "observed" properties of the Δ ($E_R=1232$ MeV and the width $\Gamma=110$ MeV). In a nuclear environment this vacuum dressing, Σ^d, is attenuated because the virtual coupling to *bare* nucleons becomes a coupling to *dressed* nucleons with Pauli blocking and, moreover, there is an additional self-energy contribution, Σ^m, which is specific for the nuclear medium (see Sec. II).

We show results for each contribution separately. In Fig. 4 the values Σ^d are displayed at normal and twice normal nuclear density and are compared with the vacuum results (solid line). One observes a reduced width of the Δ ($\Gamma/2=\text{Im}\Sigma$) which is mainly affected by the Pauli blocking on the virtual πN state. The medium Δ self-energy, Σ^m, is presented in Fig. 5 as a function of k_F. It is seen that Σ^m is much smaller in magnitude than the nucleonic values, Σ^s and Σ^0. Also, the imaginary part is very small. The resulting "effective" Δ mass can be obtained by looking at the poles of the corresponding dressed Δ Green's function. These are indicated by arrows in Fig. 4. The combined effect of Σ^d and Σ^m on the Δ effective mass does not change very much from the vacuum case ($m_\Delta=1230$ MeV). At the density $\rho=\rho_0$, we have an effective Δ mass, $m_\Delta=1200$ MeV, and at $\rho=2\rho_0$, $m_\Delta=1250$ MeV. On the other hand, the imaginary part of the effective mass, Γ, is very sensitive to the density, so that at larger densities the Δ (at rest) becomes a very stable particle. (The decay channel $\Delta\rightarrow\pi+N$ is fully quenched by the Pauli blocking.) The small effect of density on the Δ mass might be surprising compared to the large density dependence of the nucleon effective mass m^*. This is, however, not a correct comparison. Instead one should compare s_Δ, which is the Δ effective energy, to the nucleon single-particle energy. For a nucleon at rest this yields $E_{\text{s.p.}}(k=0)=m_N+\Sigma_s-\Sigma_0$. At normal density the resulting shift is only about 70 MeV downwards and at $\rho=3\rho_0$ there is even an upwards shift of $E_{\text{s.p.}}$ compared to the nucleon vacuum mass of about 30 MeV.

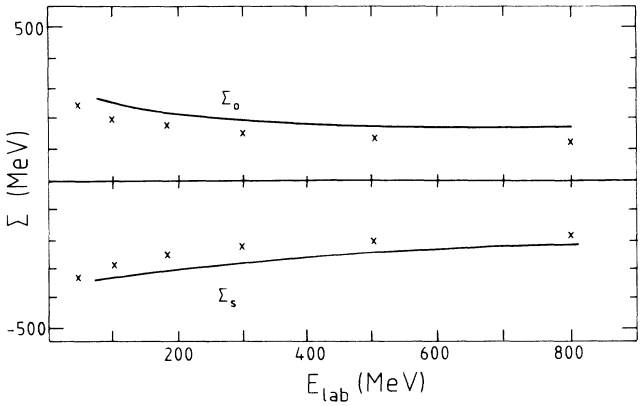

FIG. 3. Nucleon self-energy contributions Σ_s and Σ_0 vs laboratory energy. Solid lines give our Dirac-Brueckner results. The crosses represent calculations by Tjon and Wallace (Ref. 17).

B. Effective cross sections for nucleon-nucleon elastic and inelastic scattering: Pion production

In this section nucleon energies below and above the pion threshold (~300 MeV) will be considered. When discussing two-body properties in nuclear matter, we

TABLE I. The nucleon self-energy at high momenta.

P_{lab}	Σ_s		Σ_0		Σ_v		U		$E_{s.p.}$
	Re	Im	Re	Im	Re	Im	Re	Im	
(GeV/c)	(GeV)		(GeV)		(−)		(MeV)		(MeV)
			$\rho=\frac{1}{2}\rho_0$ [$k_F=0.21$ (GeV/c), $m^*=0.720$ (GeV/c^2)]						
0.45	−0.204	0.004	−0.157	0.013	−0.011	0.003	−25	−9	77
0.65	−0.180	0.009	−0.131	0.018	−0.005	0.003	−15	−11	188
0.85	−0.166	0.013	−0.113	0.021	−0.003	0.003	−7	−15	320
1.05	−0.156	0.018	−0.100	0.024	−0.002	0.003	0	−18	469
1.25	−0.151	0.019	−0.092	0.026	−0.002	0.002	4	−25	628
1.45	−0.146	0.022	−0.086	0.028	−0.002	0.002	9	−31	797
1.65	−0.142	0.026	−0.082	0.030	−0.001	0.001	14	−37	973
			$\rho=\rho_0$ ($k_F=0.26$, $m^*=0.605$)						
0.45	−0.325	0.015	−0.253	0.023	−0.023	0.007	−33	−9	69
0.65	−0.300	0.019	−0.220	0.031	−0.013	0.006	−17	−16	186
0.85	−0.278	0.025	−0.191	0.038	−0.007	0.006	−5	−26	322
1.05	−0.264	0.030	−0.171	0.044	−0.005	0.006	7	−36	476
1.25	−0.254	0.035	−0.158	0.048	−0.004	0.006	16	−47	640
1.45	−0.245	0.041	−0.150	0.053	−0.003	0.004	26	−61	814
1.65	−0.239	0.046	−0.144	0.056	−0.002	0.003	35	−73	994
			$\rho=2\rho_0$ ($k_F=0.33$, $m^*=0.428$)						
0.45	−0.515	0.014	−0.445	0.019	−0.068	0.003	0	−6	102
0.65	−0.477	0.040	−0.387	0.055	−0.038	0.007	22	−26	225
0.85	−0.446	0.049	−0.337	0.071	−0.019	0.011	38	−50	365
1.05	−0.427	0.057	−0.307	0.088	−0.012	0.014	55	−77	524
1.25	−0.413	0.063	−0.289	0.100	−0.008	0.014	72	−108	696
1.45	−0.400	0.070	−0.279	0.109	−0.007	0.014	89	−139	877
1.65	−0.391	0.076	−0.269	0.115	−0.005	0.013	101	−168	1060
			$\rho=3\rho_0$ ($k_F=0.38$, $m^*=0.309$)						
0.45	−0.649	0.008	−0.662	0.013	−0.121	0	111	−5	213
0.65	−0.574	0.031	−0.545	0.064	−0.080	0.019	103	−36	306
0.85	−0.547	0.054	−0.492	0.113	−0.043	0.023	128	−86	455
1.05	−0.526	0.067	−0.453	0.125	−0.025	0.020	150	−118	618
1.25	−0.506	0.080	−0.430	0.153	−0.017	0.027	169	−176	793
1.45	−0.489	0.084	−0.426	0.158	−0.017	0.026	192	−214	980
1.65	−0.473	0.088	−0.415	0.177	−0.018	0.026	202	−273	1161

shall use the concept of *effective cross sections.* In the following discussion, four different cross section values are distinguished. The free NN cross section, which in our approach is related to the vacuum t matrix T_{11}, will be called σ_4. In some kinetic equations, like the VUU equation, this cross section is corrected for Pauli blocking in the outgoing channel. We shall call this value σ_3. Calculating the effective cross section from the effective Dirac-Brueckner interaction, Γ_{11}, we obtain σ_1 and σ_2. Here, σ_2 is not corrected for Pauli blocking in the outgoing channel (but Pauli-blocking in the intermediate NN channels is included); σ_1 is the effective cross section that contains all medium corrections. The incoming NN channel is the same for all four cross sections. Particle 1 has a certain fixed momentum compared to the surrounding nuclear medium. For particle 2, all the available Fermi sea momenta are taken into account and averaged afterwards. In summary,

$$\sigma_1(k_1)=\frac{3}{4\pi^2 k_F^3}\int_0^{k_F} d^3k_2\,\bar{Q}(P,s^*,p)\,\frac{m^{*4}(\hbar c)^2}{2(2\pi)^2 s^*}\times\int d\Omega_{\text{c.m.}}\sum_{\sigma,\tau}|\,\Gamma_{11}(P,s^*,p)\,|^2\,, \tag{3.3}$$

where $\mathbf{P}=\mathbf{k}_1+\mathbf{k}_2$, $s^*=(E_1^*+E_2^*)^2-\mathbf{P}^2$, and $P=\frac{1}{2}(s^*)^{1/2}-4m^{*2}$, and $\sum_{\sigma,\tau}$ represents the summation (average) of outgoing (incoming) spin and isospin channels. The kinematic factor is related to our choice of the Dirac-spinor normalization: $\bar{u}(k^*)u(k^*)=1$. The function $\bar{Q}$ gives the angle-averaged Pauli-blocking operator and k_F denotes the Fermi momentum. It will be clear from above how the other values $\sigma_i(k_1)$ can be obtained. The value for σ_2, for example, can be calculated from Eq. (3.3) by ignoring the $\bar{Q}$ operator. Results are presented in Table II for $\rho=\frac{1}{2}\rho_0$, ρ_0, and $2\rho_0$, where ρ_0 is

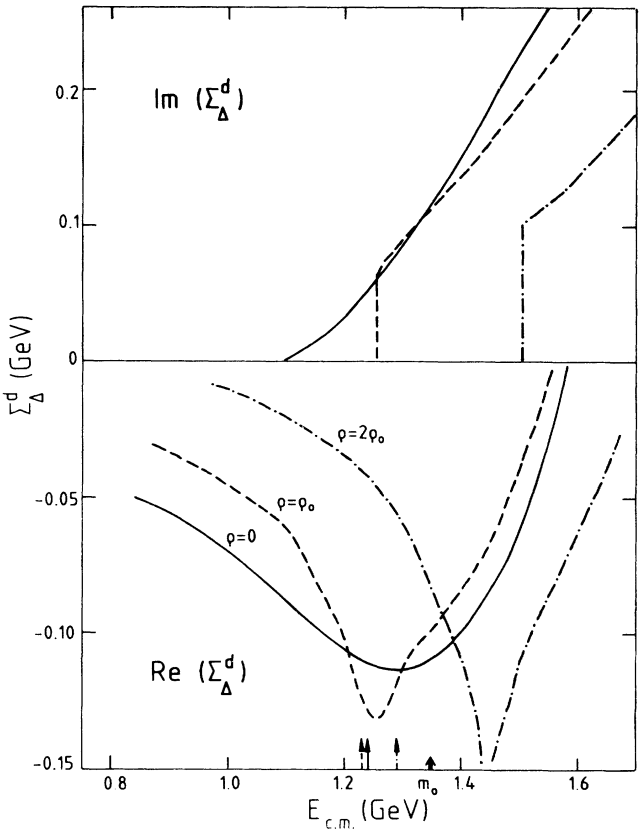

FIG. 4. The medium dependence of the decay self-energy of the Δ. The solid curve gives the vacuum results. The dashed line represents the self-energy at normal nuclear density. The dashed-dotted line represents the results at twice normal nuclear density. The arrows indicate the pole positions of the Δ propagator and correspond to the Δ effective mass. As a reference m_0 indicates the bare vacuum mass.

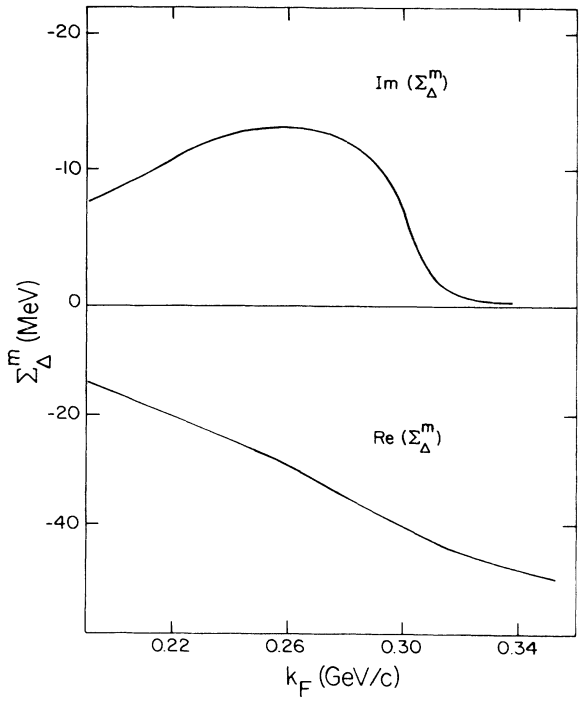

FIG. 5. The Brueckner contribution to the self-energy of the Δ vs nuclear matter density, expressed by k_F. The real and imaginary components are displayed separately.

the calculated (and empirical) saturation density. For completeness, not only the momentum of particle 1 is given, but also the energy. It is seen from this table that, especially at low energies, the effective cross sections are dramatically reduced by the combination of the two effects that we distinguish here, i.e., the use of the effective interaction, Γ_{11} (instead of the free t matrix), and the Pauli blocking in the two-particle exit channel. The importance of the first of these effects is also demonstrated in Fig. 6. Here the dashed line represents σ_3, in which only the Pauli blocking is incorporated, and the solid line represents σ_1. One sees that for the low energies and low densities, which mainly is the domain of ordinary nuclear physics, the Pauli-blocking effect dominates. But for nucleon energies in the range of 100–200 MeV, effective cross sections are very considerably reduced compared to the Pauli-blocked free ones. The effect diminishes for larger energies. The reader might prefer to think in terms of a mean free path instead of an effective cross section. Defining the mean free path λ by $\lambda=1/(\rho\cdot\sigma_1)$, we obtain, for nucleon energies above 100 MeV, values of about 5–6 fm, in agreement with empirical values.[7] Similar results, but in a more conventional approach, and for energies below the pion production threshold only, are found by the Liegé group.[19]

With respect to the effective (elastic) NN cross sections at high energies, the results differ considerably compared to the low-energy region. At high momenta the Pauli blocking becomes less and less important, and furthermore, the effective interaction, Γ_{11}, gets larger compared to the free t matrix. This is nicely demonstrated in Fig. 7, where the differential effective elastic cross section $d\sigma_2/d\Omega$ is displayed at several incoming momenta. At $p=0.85$ GeV/c one sees that for 3 times normal density the cross section is enhanced compared to results for $\rho=\rho_0$. At still higher momenta the effective cross sections are mainly left unchanged, or are even a little larger, when compared to the vacuum values. The results for the total cross sections are summarized in Table III. In this table the values for the pion production cross sections are also given. These are calculated from the effective $NN\rightarrow N\Delta$ interaction, Γ_{12}, combined with a final decay of the delta into a pion and a nucleon. Results are displayed in Fig. 8. One observes a completely opposite behavior compared to the elastic cross sections. The effective pion production cross section, σ_π, is stable at low momenta, but strongly reduced at higher values. The stability at the lower side is due to Fermi motion. Recall that we averaged over all momenta inside the Fermi sea. As a result, the inelastic channel, which is still closed in the vacuum for $p=0.5$

TABLE II. Values of effective isospin averaged NN cross sections. (k gives momentum of particle 1 in nuclear matter rest frame. $E_{s.p.}$ gives single-particle energy of particle 1, and particle 2 is integrated over Fermi sea of nuclear matter). σ_1 is the effective Dirac-Brueckner cross section, including Pauli blocking; σ_2 is σ_1 without Pauli blocking in the outgoing channel; σ_3 is the free NN cross section, with Pauli blocking in the outgoing channel; and σ_4 is the free NN cross section without Pauli blocking.

ρ/ρ_0	k (GeV/c)	$E_{s.p.}$ (MeV)	σ_1	σ_2 (mb)	E_{free} (MeV)	σ_3	σ_4 (mb)
0.5	0.22	−21.7	2.9	137	25	5.7	279
	0.25	−13.5	12.5	133	33	22.1	222
	0.29	−0.8	28.6	119	44	41.5	155
	0.31	7.3	33.7	108	50	46.7	133
	0.38	41.3	31.8	61.0	74	45.8	83.3
	0.46	81.2	23.4	35.0	107	38.5	56.8
	0.55	129.1	18.7	24.8	149	31.8	41.6
	0.65	188	17.0	20.9	203	27.4	33.3
	0.75	252	16.5	19.3	263	24.2	28.1
	0.85	213	16.4	18.7	327	22.0	24.7
1.0	0.27	−20.3	0.2	49.8	38	0.7	190
	0.29	−12.9	1.7	46.6	44	5.0	169
	0.31	−6.1	3.4	45.0	50	11.5	144
	0.34	7.2	6.6	40.2	60	21.5	115
	0.38	25.9	9.6	34.7	74	27.5	88.5
	0.42	46.1	11.6	29.9	90	29.9	70.6
	0.46	68.7	11.7	24.4	107	29.8	58.8
	0.55	122	11.9	19.5	149	27.0	42.4
	0.65	185	12.3	17.7	203	24.4	33.6
	0.75	253	13.3	17.6	263	22.1	28.2
	0.85	325	14.3	18.0	327	20.5	24.8
2.0	0.34	50	0.0	22.6	60	0.2	126
	0.38	68	0.8	22.1	74	4.0	99.1
	0.46	108	4.0	20.8	107	16.2	63.2
	0.55	159	7.3	19.9	149	19.6	44.0
	0.65	225	10.0	20.0	203	19.8	34.2
	0.75	295	12.5	21.2	263	19.0	28.4
	0.85	365	14.1	21.6	327	18.2	24.9

GeV/c, can be attained for the same momentum at densities $\rho \geq 2\rho_0$. At high momenta, far above the threshold value, pion production in nuclear matter assumes much lower values than compared to the vacuum. At $\rho = 2\rho_0$, σ_π reduces to only 40% of the vacuum value, and at $3\rho_0$ this even goes back to 25%, reaching values of only 5 mb. The absolute values of σ_π should be treated with a little caution since we underpredict (in our model) the vacuum values by 15%.[10] This factor will probably be about the same in nuclear matter. Part of the medium reduction of σ_π is due to Pauli blocking in the exit channel. Evidently, the nucleons lose energy and momentum be creating the pion, which enhances the importance of the Pauli blocking at high incoming momentum. But this only explains part of the result. Also, the effective interaction Γ_{12} is reduced, mainly because of the low values of the effective nucleon mass m^* that are involved. These effectively reduce the $N\Delta\pi$ coupling. Interfering with ρ exchange, this results in the observed quenching of σ_π. Evidently, the observed density dependence of the pion production cross section has interesting consequences for the description of pion yields in relativistic heavy ion collisions. One might recall that until now, the model calculations overpredicted the number of final pions.[1,2] Figure 8 indicates why, in part, but not fully, since the density dependence of the pion absorption mechanism might also strongly influence the number of produced pions. It is clear that an enhanced absorption rate might have the same effect as a reduced production rate. We shall allude to this problem in the next section.

IV. DELTA ABSORPTION AND ELASTIC SCATTERING IN NUCLEAR MATTER

In this section we shall present calculations of the remaining effective interactions, Γ_{21} and Γ_{22}. In contrast to the preceding section, the incoming channel consists, in this case, of a nucleon and a delta. The results that we obtained here should be viewed with a little more caution than those of the foregoing section. The reason for this is that, empirically as well as theoretical-

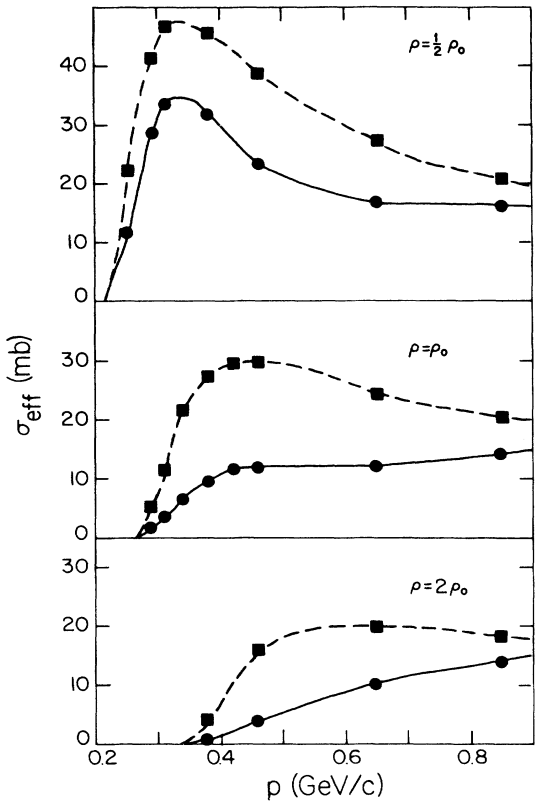

FIG. 6. Effective elastic nucleon-nucleon cross sections as a function of nucleon momentum in the laboratory system, for densities $\rho=\frac{1}{2}\rho_0$, ρ_0, and $2\rho_0$, where ρ_0 gives the saturation density. Dirac-Brueckner results (solid lines) are compared with calculated free cross sections corrected for Pauli blocking on the final phase space population (dashed lines).

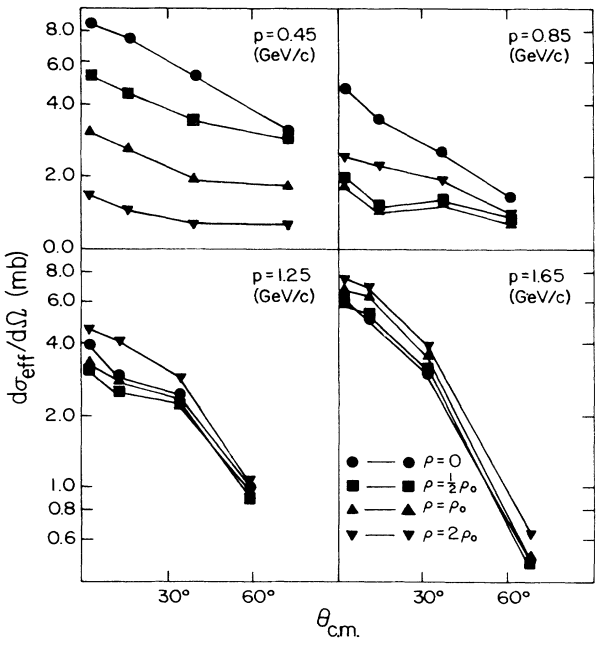

FIG. 7. Effective differential elastic NN cross sections calculated in the Dirac-Brueckner approach as a function of c.m.-scattering angle $\theta_{c.m.}$ for different (laboratory) nucleon momenta and different nuclear densities.

TABLE III. The effective elastic and pion production cross section.

p_{lab} (GeV/c)	$E_{s.p.}$ (MeV)	σ_1 (mb)	σ_2 (mb)	σ_π (mb)
$\rho=\frac{1}{2}\rho_0$	$[k_F=0.21$ (GeV/c),	$m^*=0.720$ (GeV/c^2)]		
0.45	77	24.1	37.0	0.0
0.65	188	17.0	20.9	0.2
0.85	320	16.4	18.7	1.3
1.05	469	16.2	17.7	4.3
1.25	628	16.3	17.5	8.9
1.45	797	16.8	17.7	12.7
1.65	973	17.7	18.5	14.7
	$\rho=\rho_0$	$(k_F=0.26,$	$m^*=0.605)$	
0.45	67	11.8	24.7	0.0
0.65	185	12.3	17.7	0.2
0.85	325	14.3	18.0	1.6
1.05	476	15.3	17.7	4.5
1.25	640	16.4	18.5	8.0
1.45	814	17.5	19.2	10.6
1.65	994	18.8	20.3	11.8
	$\rho=2\rho_0$	$(k_F=0.33,$	$m^*=0.428)$	
0.45	102	4.0	20.8	0.0
0.65	225	10.0	20.0	0.3
0.85	365	14.1	21.6	2.2
1.05	524	15.8	21.2	4.7
1.25	696	17.7	22.2	6.2
1.45	877	19.3	23.0	7.1
1.65	1060	20.8	24.0	7.9
	$\rho=3\rho_0$	$(k_F=0.38,$	$m^*=0.309)$	
0.45	213	2.0	25.2	0.1
0.65	305	8.3	23.3	0.4
0.85	448	13.5	24.7	1.8
1.05	623	16.2	24.8	3.6
1.25	785	18.4	25.7	4.5
1.45	976	20.4	26.7	4.6
1.65	1161	21.6	27.2	4.8

ly, very little is known about the NΔ interaction. This is reflected in large uncertainties concerning the OBE interaction V_{22}, which is not very important in the NN effective interaction, but its role is increased in the NΔ interaction. Furthermore, in our approach we ignored possible intermediate ΔΔ states. This also reduced the

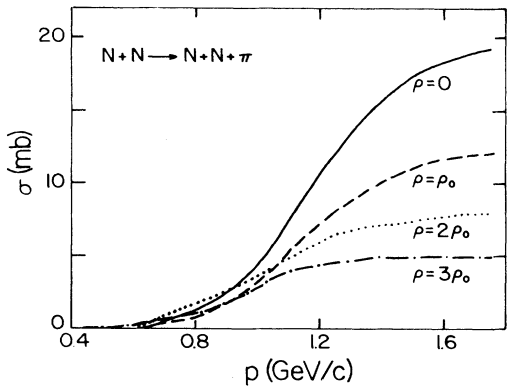

FIG. 8. Effective pion production cross sections vs nucleon momentum in the laboratory system for different nuclear densities.

trustworthiness of our calculations for the NΔ interaction. Finally, our nuclear matter approach accounts only for an infinite system of nucleons. The possibility of a certain mixture of nucleons and deltas with both their own characteristic density is fully ignored. In realistic calculations, however, one might deal with a finite delta/nucleon ratio. This would cause additional couplings (although they are probably less important) that are not included here. In this section we describe properties of a single delta interacting with nucleons which are part of a purely nucleonic medium. For the incoming channel of Γ_{21} and Γ_{22} we chose the nucleon to be at rest in the nuclear medium, and we varied the Δ momentum. The incoming (invariant) Δ mass, s_Δ, has been fixed at the value of $s_\Delta = 1.23$ GeV. Note that in the nuclear medium this is not the on-shell value for all densities. Concurrently, we could have chosen the density-dependent on-shell value of s_Δ as the starting energy, but the differences are not very large. As we have shown in Sec. III A, the Δ mass shifts to somewhat lower values than the vacuum mass, 1.23 GeV/c^2, at low densities, but at densities higher than normal density this effective mass moves upwards, but to values still smaller than 1.3 GeV/c^2 at $\rho = 3\rho_0$. However, since one is more interested in pion absorption than Δ absorption, the on-shell Δ mass is of somewhat less importance. As we checked explicitly, the influence of s_Δ on the final results is small, and is mainly reflected in the Pauli blocking in the exit channel.

As in Sec. III, we calculated effective cross sections based on Γ_{21} and Γ_{22}, and incorporated Pauli blocking in the exit channel. To calculate the Pauli-blocking factor, we relaxed the initial condition (nucleon at rest in the medium), and averaged over the nucleon states in the Fermi sea. Practically, this diminishes the effect of Pauli blocking somewhat, but gives, in our opinion, a better view of what Pauli blocking, in realistic cases, might do. Note that a nucleon at rest in nuclear matter is very rare, although the average momentum (not as a length but as a vector) is zero. Results for the Δ absorption cross section, $\sigma(N\Delta \rightarrow NN)$, are presented in Fig. 9, where the vacuum values ($\rho = 0$) are compared to values in dense nuclear matter, $\rho = \rho_0$, $2\rho_0$, and $3\rho_0$. In contrast to some speculations about enhanced Δ absorption in nuclear matter,[18] one observes a reduction of the effective cross section as a function of density. Because of the mass difference between the incoming and outgoing channels, the outgoing momenta are rather large, which reduces the effect of Pauli blocking for $\rho \leq 2\rho_0$ considerably. At $\rho = \rho_0$ the effect of Pauli blocking in the exit channel is negligible. The difference between $\sigma(\rho_0)$ and $\sigma(2\rho_0)$ is half caused by Pauli blocking and half explained by a reduction of Γ_{21}. The striking reduction at $\rho = 3\rho_0$ is, however, to a large extent the result of Pauli blocking. The mass difference yields a momentum gain that is smaller than the Fermi momentum at this density. In this respect the Δ absorption cross section behaves differently from the elastic NΔ cross section, which is displayed in Fig. 10. Here, already at normal density, the low-momentum results are strongly reduced, in part by the blocking of the outgoing channel. In fact,

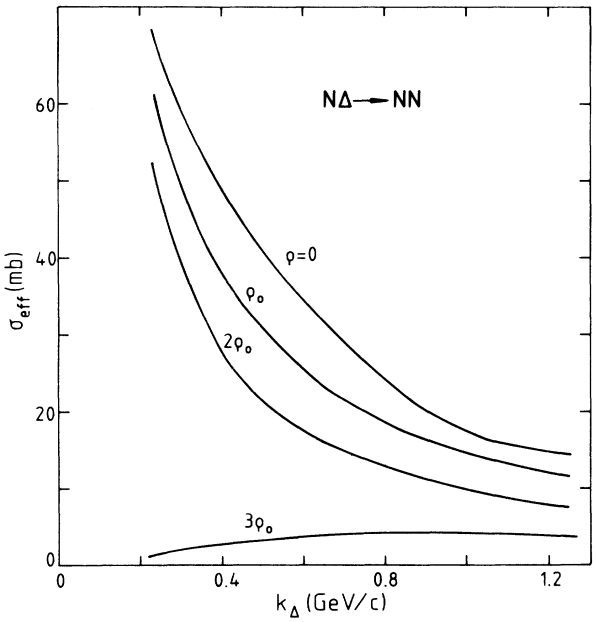

FIG. 9. Effective Δ-absorption cross sections as a function of laboratory Δ momentum for different nuclear densities (ρ_0 represents the nuclear saturation density).

Fig. 10 largely resembles the effective elastic NN cross sections, shown in Fig. 6. As a result, for Δ momenta below 0.7 GeV/c, the Δ absorption, although in absolute terms reduced, is strongly enhanced relative to Δ elastic scattering, compared to the vacuum situation. For higher momenta, the behavior is the opposite and the Δ absorption is more severely reduced than the elastic

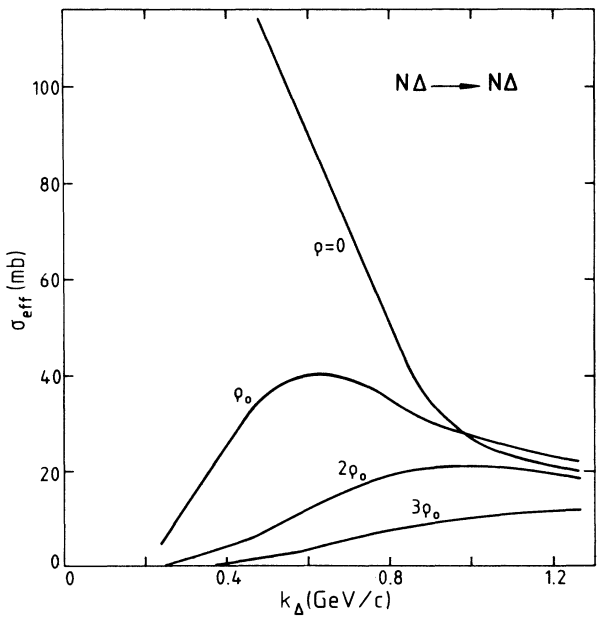

FIG. 10. Effective ΔN elastic cross sections as a function of laboratory Δ momentum for different nuclear densities.

scattering. Even though the cross section values, in an absolute sense, contain large uncertainties, we believe that the trends observed here are rather unambiguous.

V. SUMMARY

We have discussed high-energy nucleon and delta properties in dense nuclear matter. These properties are of great importance in proton-nucleus, pion-nucleus, and nucleus-nucleus scattering. We opted for a fully-self-consistent approach, built on field theory, which combines an adequate description of all the vacuum properties of nucleons, deltas, and their scattering processes with an equally good description of the empirically known properties of nuclear matter. The resulting Dirac-Brueckner approach for nucleons and deltas has been applied here to situations of large particle momenta. For highly-energetic nucleons, we calculated the self-energy decomposed into its scalar and vector components. The resulting values are in agreement with values obtained empirically or theoretically, by using the relativistic impulse approximation in the study of proton-nucleus scattering. Since these approaches differ considerably, particularly with respect to self-consistency and the treatment of negative-energy nucleon states, these points need more attention in future calculations. The (generally) nonlocal self-energy can also be approximated in terms of a local mean field. It turns out that this mean field becomes repulsive both for large momenta as well as for large densities. This momentum dependence has been overlooked in most of the calculations of the equation of state derived from nucleus-nucleus collisions. In the presentation of our results we focus on the concept of effective, medium-dependent cross sections, which are related to the effective Dirac-Brueckner interaction, Γ, instead of the free t matrix. This correction to the vacuum cross section exists in addition to the more frequently used Pauli-blocking effect in the outgoing two-particle channel. For the elastic NN interaction we observe, in the energy range 50–400 MeV, a strong reduction of the effective cross section, which is only in part due to Pauli blocking. For higher energies the difference compared to the vacuum cross section becomes much smaller and even changes sign. The effective inelastic NN interaction determines mainly pion production in a nuclear medium. It is seen that although, through Fermi motion, the production threshold shifts downwards, at high momenta the inelastic channel is strongly decreasing as a function of density. This indicates a mechanism that is responsible for the fact that the observed pion yield in relativistic nucleus-nucleus collisions is considerably smaller than calculations have so far predicted. On the other hand, the final number of produced pions depends also on pion absorption of the medium. To attack this problem, we calculated Δ absorption and Δ elastic scattering in dense nuclear matter. Both turn out to decrease as a function of density for Δ momenta below 0.7 GeV/c. Relative to elastic scattering, however, the importance of Δ absorption is enhanced considerably. For higher momenta the situation is the opposite.

All the foregoing novel results might be interesting in themselves. More important, however, is an implementation of our concepts and results in realistic particle-nucleus and nucleus-nucleus calculations, in which they eventually can be verified. In this respect, the situation in which the temperature takes on finite values (i.e., dense and hot nuclear matter) also needs further study.

[1]R. Stock, Phys. Rep. **135**, 259 (1986).
[2]R. Stock *et al.*, Phys. Rev. Lett. **49**, 1236 (1982); J. W. Harris *et al.*, *ibid.* **58**, 463 (1987).
[3]H. Stöcker and W. Greiner, Phys. Rep. **137**, 277 (1986).
[4]J. Boguta, Phys. Lett. **106B**, 250 (1981).
[5]B. ter Haar and R. Malfliet, Phys. Lett. **172B**, 10 (1986).
[6]C. Gale, G. Bertsch, and S. Das Gupta, Phys. Rev. C **35**, 1666 (1987); J. Aichelin, A. Rosenhauser, G. Peilert, H. Stöcker and W. Greiner, Phys. Rev. Lett. **58**, 1926 (1987).
[7]J. W. Negele and K. Yazaki, Phys. Rev. Lett. **47**, 71 (1981); H. O. Meyer and P. Schwandt, Phys. Lett. **107B**, 353 (1981).
[8]W. Botermans and R. Malfliet, Phys. Lett. **171B**, 22 (1986); R. Malfliet, B. ter Haar, and W. Botermans, J. Phys. (Paris) Colloq. **47**, C2-287 (1987).
[9]B. C. Clark *et al.*, Phys. Rev. C **28**, 1421 (1983).
[10]B. ter Haar and R. Malfliet, Phys. Rep. **149**, 207 (1987).
[11]D. Ashery and J. P. Schiffer, Annu. Rev. Nucl. Part. Sci. **36**, 207 (1986).
[12]B. D. Serot and J. D. Walecka, Adv. Nucl. Phys. **16**, 1 (1986).
[13]M. R. Anastasio, L. S. Celenza, W. S. Pong, and C. M. Shakin, Phys. Rep. **100**, 327 (1983).
[14]R. Brockmann and R. Machleidt, Phys. Lett. **149B**, 283 (1984).
[15]E. E. H. van Faassen and J. A. Tjon, Phys. Rev. C **30**, 285 (1984).
[16]J. A. McNeil, J. R. Shepard, and S. J. Wallace, Phys. Rev. Lett. **50**, 1439 (1983); J. R. Shepard, J. A. McNeil, and S. J. Wallace, *ibid.* **50**, 1443 (1983).
[17]J. A. Tjon and S. J. Wallace, Phys. Rev. C **32**, 267 (1985).
[18]G. E. Brown and P. J. Siemens (unpublished).
[19]A. Lejeune, P. Grangé, M. Martzolff, and J. Cugnon, Nucl. Phys. **A453**, 189 (1986).